10.051103/RES.260605105

Vol.5 Iss.1 pp.47-60 International Journal of Renewable Energy and Sustainability (RES)

Processor-In-the-Loop Implementation for PSO MPPT Control and Backstepping Technique for a Photovoltaïc System

Hajar Dammah#1, Nabil Arsalane#, Bouassam Hamid#, Omar Cherrak#

 # 1LMSI Lab, International University of Casablanca, Casablanca 8118, Morocco

1 hajar.dammah@uic.ac.ma

Abstract— **This paper considers the problem of controlling a single-phase grid-connected photovoltaic system using the Particle Swarm Optimization (PSO) algorithm and the backstepping as a nonlinear control technique. The studied system includes a PV panel, a DC-DC Boost converter, a DC-AC half-bridge inverter, and an L filter to connect the system to the grid. The PSO algorithm is employed to determine the Maximum Power Point Tracking (MPPT) by optimizing the power extraction from the PV panel. This work aims at achieving threefold control objectives: i) extracting the maximum available power using the PSO algorithm, ii) guaranteeing a unitary power factor (UPF) by forcing the grid current to be sinusoidal and in phase with the electric network voltage, and iii) regulating the DC link voltage to a desired reference value. A stability analysis of the voltage regulation loop, power extraction, and power factor control loops will be addressed. The performance of the proposed controller is evaluated through numerical simulations using the MATLAB/SIMULINK environment and validated through a Processor-in-the-Loop implementation.**

Keywords— **PSO Algorithm, MPPT, PV System, Processor-in-the-Loop, Backstepping**

I. INTRODUCTION

The demand for electrical energy is increasing day by day, and this energy is largely produced via fossil fuels which represents many disadvantages. However, a transition to green energy is necessary. Currently, several renewable energy sources are used in the development of the energy sector due to their clean and sustainable characteristics. However, in this article, the exploitation of photovoltaic (PV) energy turns out to be an ideal solution, as it is abundant given the geolocation of the country, renewable and free.

In order to exploit the photovoltaic panels to the power grid, a matching stage is required to achieve two main objectives: extracting the maximum power and injecting the current with a unity power factor. The DC-DC Boost converter is often chosen for this purpose due to its simplicity and high efficiency [1]. This converter ensures that the PV module operates at its maximum power point (MPP).

In order to optimize the power generation efficiency of photovoltaic panels, MPPT technology has attracted several research works, because the output characteristic curve of the photovoltaic array is nonlinear due to the influence of light, temperature, etc. Therefore, it is crucial to propose a suitable MPPT control method [2][11]. However in this paper we propose the use of the PSO (Particle Swarm Optimization) algorithm. PSO, inspired by nature and more precisely by the collective behavior of swarms [3], is a robust optimization method that dynamically adjusts the reference voltage by exploring the search space to maximize the power delivered by the PV panels. Each particle represents a voltage and evolves according to its individual best position (personal best) as well as the global best position obtained by all particles, allowing a fast and accurate convergence towards the MPP, even under variable solar conditions.

To connect the conversion system with the grid, inverters are used. Adaptive approaches for AC and DC systems have also been explored in the literature. For example, [4] introduced a sliding mode controller (SMC) combined with an adaptive observer to improve the robustness and performance of the system with INC algorithm. Similarly, [5] proposed a control law using the backstepping approach to stabilize the overall system with a P&O algorithm.

The work reported in this paper focuses on the analysis of a grid-connected PV system using a PSO algorithm to ensure maximum power point tracking and a nonlinear controller based on the Backstepping technique to ensure the control objectives. The system integrates three control loops: i) maximum power point tracking (MPPT) using the PSO algorithm, ii) regulating the DC bus voltage, iii) obtaining a unity power factor in order

ISSN: 2961-6603

to inject a current in phase with the voltage into the grid. In addition, the Lyapunov technique for stability analysis will be performed to ensure the asymptotic stability of the closed-loop system. Finally, the use of a half-bridge inverter which offers several advantages, including lower costs due to a reduced number of switching components and the possibility of doubling the output current compared to a full-bridge inverter.

II. System Description and Modelling

A. System Description

The structure of the single-phase PV-powered power conversion system, as shown in Figure 1, is divided into two main parts: a DC section and an AC section. The DC section comprises a PV panel connected to a DC-DC boost converter, while the AC section, which serves as an interface with the single-phase grid, consists of a half-bridge inverter with an L filter. The DC-DC converter and the DC-AC half-bridge are controlled by the inputs μ1∈ {0,1} and μ2∈ {-1,1}, respectively. The commutations of the converters are governed by the pulse-width modulation (PWM) technique.

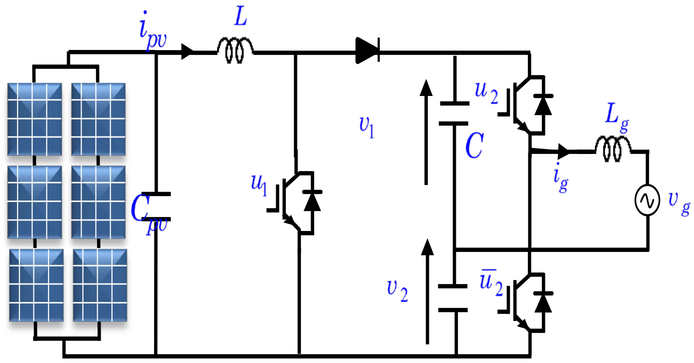

Fig. 1 Structure of the studied system

B. System Modelling

Using the standard Kirchhoff laws, the switched model of the single-phase half-bridge PV system can be obtained, as follows:

$$C_{pv}\frac{dv_{pv}}{dt} = \overline{\iota_{pv}} - i_l \tag{1.a}$$

$$L\frac{di_l}{dt} = v_{pv} - (1-\mu_1)(v_1 - v_2) \tag{1.b}$$

$$C\frac{dv_1}{dt} = (1-\mu_1)i_l - \frac{(1-\mu_2)}{2}i_g \tag{1.c}$$

$$C\frac{dv_2}{dt} = (1-\mu_1)i_l - \frac{(1-\mu_2)}{2}i_g \tag{1.d}$$

$$L_g\frac{di_g}{dt} = -r_g i_g + \frac{(1+\mu_2)}{2}v_1 - \frac{(1-\mu_2)}{2}v_2 - v_g \tag{1.e}$$

With i_{pv} is the PV current, v_{pv} the PV voltage, v_1 *and* v_2 are the capacitor voltages, i_1 is the inductor current, r_g is the equivalent series resistance of inductance L_g,
Let's put: $v_1 + v_2 = v_o$ and $v_1 - v_2 = v_d$
Or in this model μ_1 and μ_2 are a binary control inputs, therefore, it is not suitable to be based upon them while designing continuous control laws. To solve this problem, it is usually resorted to the average model.

$$C_{pv}\frac{dx_1}{dt} = \overline{\iota_{pv}} - x_2 \tag{2.a}$$

$$L\frac{dx_2}{dt} = x_1 - (1-u_1)x_3 \tag{2.b}$$

ISSN: 2961-6603

10.051103/RES.260605105
Vol.5 Iss.1 pp.47-60 **International Journal of Renewable Energy and Sustainability (RES)**

$$C\frac{dx_3}{dt} = 2(1-u_1)x_2 - u_2x_5 \quad (2.c)$$

$$C\frac{dx_4}{dt} = -x_5 \quad (2.d)$$

$$L_g\frac{dx_5}{dt} = -r_gx_5 + \frac{1}{2}x_4 - \frac{u_2}{2}x_3 - v_g \quad (2.e)$$

TABLE I.
AVERAGE VALUES OF MODEL

Parameter	symbols	average values
PV voltage	v_{pv}	x_1
PV Current	i_{pv}	$\bar{i}_{pv}$
Inductor current	i_l	x_2
Sum voltage of v_1 and v_2	v_o	x_3
Differential voltage of v_1 and v_2	v_d	x_4
grid current	i_g	x_5
Binary input control	μ_1	u_1
Binary input control	μ_2	u_2

III. PARTICLE SWARM OPTIMIZATION ALGORITHM FOR MAXIMUM POWER POINT TRACKING

The goal of MPPT algorithms is to maximize the power extracted from photovoltaic (PV) panels. In this work, the Particle Swarm Optimization (PSO) algorithm is used. It is an intelligent algorithm widely used in various optimization problems. This algorithm is inspired by nature, and more precisely by the collective behaviours of swarms, such as birds or fish gathering [6] [9].

The PSO algorithm, is based on randomly distributed particles in the M-dimensional search space [7] [8], whose $X_i = (x_{i1}, x_{i2}, \dots, x_{iM})$ is a solution to the optimization problem in the M-dimensional space, corresponding to the position of the i^{th} particle in the particle swarm. While $P_{ibest} = (p_{i1}, p_{i2}, \dots, p_{iM})$ is considered as the optimal position on all paths travelled by the i^{th} particle, it is the best local optimal solution sought. However, $Gbest = (G_{best1}, G_{best2} \dots, G_{bestm})$ represents the optimal position on the path travelled by all the particles, it means the global optimal solution. $V_i = (v_{i1}, v_{i2}, \dots, v_{iM})$ is the velocity of the particle. Relations represent by (3) and (4) are the main formulas of the PSO, and particles update their positions and velocities using these two formulas.

$$v_{i+1} = w * v_i + c_1rand_1(P_{best} - x_i) + c_2rand_2(G_{best} - x_i) \quad (3)$$

$$x_{i+1} = x_i + v_i \quad (4)$$

To apply this algorithm shown in figure 2, in the context of MPPT, each particle in the swarm represents a value of the candidate voltage, and its fitness function corresponds to the output power of the PV system. The particles iteratively adjust their positions (voltages) according to their own best performance (Pbest) and the best overall performance observed within the swarm (Gbest). This approach promises convergence and better adaptability to dynamic environmental changes, such as variations in solar irradiance and temperature. Compared to conventional MPPT methods such as Perturb and Observe (P&O) or Incremental Conductance, the PSO algorithm offers improved accuracy and stability, especially under non-uniform climate conditions. The flow chart of the PSO is shown in figure 2.

ISSN: 2961-6603

10.051103/RES.260605105
Vol.5 Iss.1 pp.47-60 International Journal of Renewable Energy and Sustainability (RES)

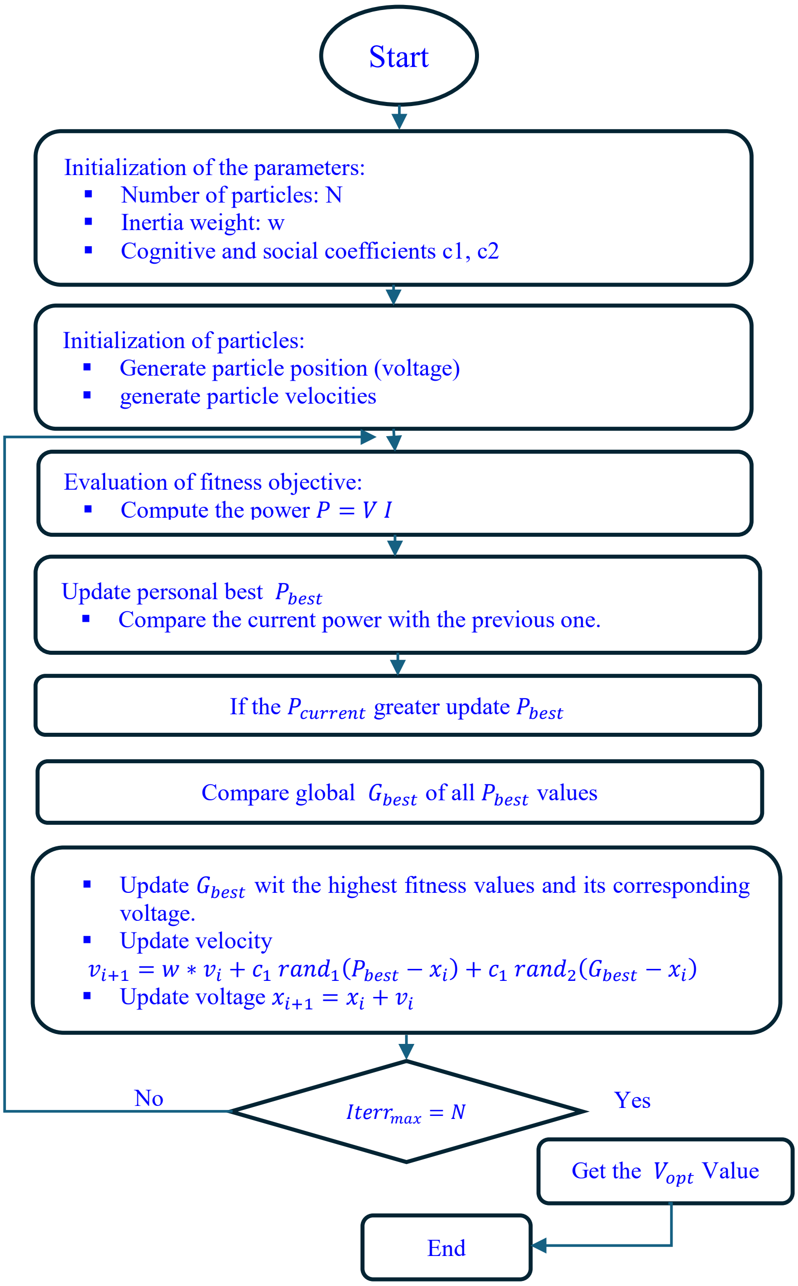

Fig. 2 Particle Swarm Optimization Flow Chart.

TABLE II.
PARAMETERS AND ITS VALUES FOR PSO ALGORITHM.

Parameter	**Symbol**	**Description**	**Value**
Number of particles	N	Total number of particles in the swarm.	10
Maximum iterations	$Iter_{max}$	Maximum number of iterations for convergence.	100
Cognitive coefficient	c1	Weight for personal best position influence.	2
Social coefficient	c2	Weight for global best position influence.	2
Inertia weight	w	Balances exploration and exploitation (adjusts velocity).	0,7

ISSN: 2961-6603

10.051103/RES.260605105
Vol.5 Iss.1 pp.47-60 **International Journal of Renewable Energy and Sustainability (RES)**

IV. CONTROLLER DESIGN

A. *Grid current and DC-link Regulator*

To achieve the above-mentioned control objectives, a controller using the Backstepping control technique [10] will be developed below. This approach ensures robust performance by adapting to system and network variations while maintaining precise control.

A multi-loop configuration will be adopted for regulator design, which will allow for better performance. The inner loop provides power factor correction (PFC). It integrates a non-linear current regulator injected into the network. The outer loop, on the other hand, consists of a filtered PI regulator, responsible for maintaining the DC bus voltage at the desired reference, thus ensuring the stability and precision of the system [13].

1) *Grid Current Regulator Design*

To ensure that the power factor correction (PFC) objective is met, the current injected into the grid must be sinusoidal and in phase with the grid voltage. This maintains efficient power transfer and minimizes harmonics. The goal of the controller is to force the grid current x_5 to follow a reference signal as follows:

$$x_5^* = \beta e_g \qquad 5$$

β is a positive real signal that helps to optimize tracking performance and ensure the desired current behaviour.

The tracking error of the grid current estimate is defined as:

$$z_1 = L_g(x_5 - x_5^*) \qquad 6$$

By differentiating z_1 with respect to time and using equation (2.e), the dynamics of the error are obtained:

$$\dot{z}_1 = -r_g x_5 + \frac{x_4}{2} + \frac{u_2}{2} x_3 - e_g - L_g \dot{x}_5^* \qquad 7$$

To analyze the stability of the error dynamics, we define the following Lyapunov candidate function:

$$V_1 = 0.5 z_1^2 \qquad 8$$

Its time derivative is given by:

$$\dot{V}_1 = -c_1 z_1^2 < 0 \qquad 9$$

where c_1 is a positive parameter that acts the convergence of the tracking error z_1. The dynamic of error is:

$$\dot{z}_1 = -c_1 z_1 \qquad 10$$

The solution of this equation is:

$$z_1(t) = z_1(0)e^{-c_1 t}$$

Where $z_1(0)$ represents the tracking error at t=0. This result implies that the system described in equation (2;e) is exponentially stable. The exponential term $e^{-c_1 t}$ ensures that the function decays rapidly with a rate determined by c_1. A larger value of c_1 results in faster convergence.

To stabilize the error, let combine (7) and (10), one obtains the following control law:

$$u_2 = \frac{2}{x_3}\left(r_g x_5 - \frac{1}{2}x_4 + e_g + L_g \dot{x}_5^* - c_1 z_1\right) \qquad 11$$

therefore, the equilibrium (z3=0) is globally asymptotically stable, and the PF unit is asymptotically reached.

2) *DC link Regulator*

In this section, the β signal serves as a control input, the purpose of which is to ensure that the square of the DC bus voltage, x_3^2 , follows a constant reference signal $(x_3^*)^2$. This reference is subject to the condition:

$$x_3^* > 2E_g \qquad 12$$

ISSN: 2961-6603

10.051103/RES.260605105

where E_g represents the peak amplitude of the grid voltage. The reference signal x_3^* defines the desired value for the DC link voltage.

It is necessary to design a control law for β that guarantees $x_3^2 \to (x_3^*)^2$, ensuring regulation of the DC bus voltage. This control law will be based on a **filtered PI regulator.**

To ensure correct control, the following assumptions are made:

1. The signal β and its first three derivatives must be available for calculation.
2. The reference $(x_3^*)^2$ is constant

The control law is expressed as:

$$\beta = \left(\frac{c_6}{c_6 + s}\right)^3 \left(-k_p e - k_i \int e\, dt\right) \quad 13$$

where:

- $e = x_3^2 - (x_3^*)^2$ is the error between the actual squared voltage and the reference squared voltage.
- $k_p > 0$ and $k_i > 0$ are the proportional and integral gains, respectively.

Theorem:

Consider the closed-loop control system composed of the following elements:

1. The system dynamics described by equations (2d-e).
2. The control law defined in (11) and (13).

The global dynamics of the closed-loop system is governed by equations above.

Under these conditions, the closed-loop system is globally asymptotically stable with respect to the Lyapunov functions defined.

B. PV Voltage Regulator Design

The control law of the DC/DC boost converter is developed using the backstepping control technique with a maximum power point tracking (MPPT) block [12]. The MPPT block works using the PSO optimization algorithm already developed earlier in this paper. The main objective of this controller is to ensure that the voltage generated by the PV system accurately follows the reference voltage provided by the PSO algorithm.

Equations (2a-b) of the average system model describe the PV-Boost subsystem, and are used to derive the control law, where u_1 represents the actual control input. And since the considered subsystem has a relative degree of two, the Backstepping technique will be used in two sequential steps. These steps analyze the system dynamics to ensure robust voltage regulation while maintaining stability and performance.

Step 1: Stabilization of Subsystem (2a)

To stabilize the subsystem described by equation **(2a)**, we introduce the following tracking error:

$$e_1 = C_{pv}(x_1 - x_1^*) \quad 14$$

Here, x_1^* represents the reference voltage given by the PSO algorithm. The goal is to achieve tracking by forcing the error e_1 to disappear, thus ensuring that the PV voltage x_1 follows its reference x_1^*.

$$\dot{e}_1 = \bar{\imath}_{pv} - x_2 - C_{pv}\dot{x}_1^* \quad 15$$

Taking the time derivative of e_1 and substituting from equation (2a), we obtained:

The error dynamics in (15) form the basis for designing a control law that ensures the stabilization of the subsystem. In equation (15), the term x_2 is considered as a virtual control variable. To analyze the stability of the system, we define the following Lyapunov candidate function:

ISSN: 2961-6603

10.051103/RES.260605105

$$W_1 = \frac{1}{2} e_1^2 \qquad (16)$$

The Lyapunov function is nothing other than the energy of the error e_1, its objective is to bring it back to zero. In the dynamics of W_1 we obtain:

$$\dot{W}_1 = e_1\left(\bar{\iota}_{pv} - x_2 - C_{pv}\dot{x}_1^*\right) \qquad (17)$$

This equation reflects the evolution of the error over time. This equation reflects the evolution of the error over time. It is necessary to determine a stabilizing function for x_2, in order to ensure that the dynamics of the Lyapunov function becomes negative definite, to ensure the convergence of the tracking error e_1 towards zero. It must be negative definite as chosen in (18):

$$\dot{W}_1 = -\lambda_1 e_1^2 \qquad (18)$$

where $c_1 > 0$ is a design parameter. Since x_2 is not the actual control input, a new error variable e_2 is between the virtual control and its desired value x_2^* is introduced:

$$e_2 = L(x_2 - x_2^*) \qquad (19)$$

With $x_2^* = \bar{\iota}_{pv} - C_{pv}\dot{x}_1^* + \lambda_1 e_1$ (20)

The next step involves determining an appropriate **control signal** u_1 to ensure that the tracking error e_1 vanishes asymptotically. To achieve this, we substitute from equations **(19)** and **(20)** into equation **(15),** which yields the following error dynamics:

$$\dot{e}_1 = -\lambda_1 e_1 - \frac{e_2}{L} \qquad (21)$$

Here:

- λ_1 is a positive parameter that contributes to the exponential decay of e_1,
- e_2 is another error variable introduced to further refine the control strategy.

To analyze the stability of the system, let consider the time derivative of the Lyapunov function W_1 along the trajectory of equation (21):

$$\dot{W}_1 = -\lambda_1 e_1^2 - \frac{e_1 e_2}{L} \qquad (22)$$

The first term, $-\lambda_1 e_1^2$, is negative definite and ensures the dissipation of the error energy e_1. However, the second term, $-\frac{e_1 e_2}{L}$, couples the errors $e_1 and\ e_2$, and is necessary to ensure the overall stability of the system. The next step will be to analyze the dynamics of e_2 to ensure the asymptotic convergence of $e_1 and\ e_2$.

Step 2: Stabilization of Subsystem (2a-b)

The next objective is to design a control strategy such that the set of errors (e_1, e_2) vanishes asymptotically. To achieve this, it is essential to analyze the dynamics of e_2. From the system equations, the time derivative of e_2 is given by (23). To analyze the stability of the error dynamics, consider the augmented Lyapunov function described in (24)

where W_1 represents the Lyapunov function introduced in Step 1. The focus now is to ensure that the time

$$\dot{e}_2 = x_1 - (1 - u_1)x_3 - L\dot{x}_2^* \qquad (23)$$

$$W_2 = W_1 + \frac{1}{2} e_2^2 \qquad (24)$$

derivative of W_2 is **negative definite,** guaranteeing the stability of the errors. Taking the derivative of W_2 along the trajectories of $e_1 and\ e_2$, we have:

$$\dot{W}_2 = -\lambda_1 e_1^2 - e_2\left(\frac{e_1}{L} - \dot{e}_2\right) \qquad (25)$$

To ensure the negativity of $\dot{W}_2$, we select $\dot{e}_2$ as follows:

ISSN: 2961-6603

10.051103/RES.260605105
Vol.5 Iss.1 pp.47-60 International Journal of Renewable Energy and Sustainability (RES)

$$\dot{e}_2 = \frac{e_1}{L} - \lambda_2 e_2 \qquad 26$$

Here:

- λ_2 is a design parameter chosen to regulate the rate of convergence of e_2,
- The first term, $\frac{e_1}{L}$, compensates for the coupling between $e_1 and\ e_2$, while the second term ensures the exponential decay of e_2.

With this choice of e_2, the time derivative of the Lyapunov function becomes:

$$\dot{W}_2 = -\lambda_1 e_1^2 - \lambda_2 e_2^2$$

This expression is **negative definite**, indicating that the equilibrium point $(e_1, e_2) = (0,0)$ is **globally asymptotically stable**. This concludes the stabilization of the error dynamics for both $e_1 and\ e_2$.
By combining equations (23) and (26), the final expression for the control input u_1 is obtained. This control law ensures the stabilization of the error variables e_1 and e_2, driving them to zero asymptotically. The derived control law is expressed as follows:

$$u_1 = 1 + \frac{Lx_2^* - x_1 - \lambda_2 e_2 + \frac{e_1}{L}}{x_3} \qquad 27$$

This control law effectively ensures that the error variables (e_1, e_2) converge to zero, stabilizing the subsystem and guaranteeing that the system's output accurately follows the reference trajectory. The proper choice of the design parameter λ_2 plays a critical role in achieving a balance between stability and responsiveness.

V. RESULTS OF THE PIL EXPERIMENT

The efficiency of PSO Algorithm and nonlinear controller proposed for Single-Phase Grid-Connected Photovoltaic System is investigated by processor in the loop (PIL) experiment using eZdsp controller board of Texas Instrument (Fig.3) parallel with MATLAB/Simulink. The PIL test was conducted under two conditions test and with a sampling frequency of 10 kHz. The parameters used in this experiment are shown in Table 3.

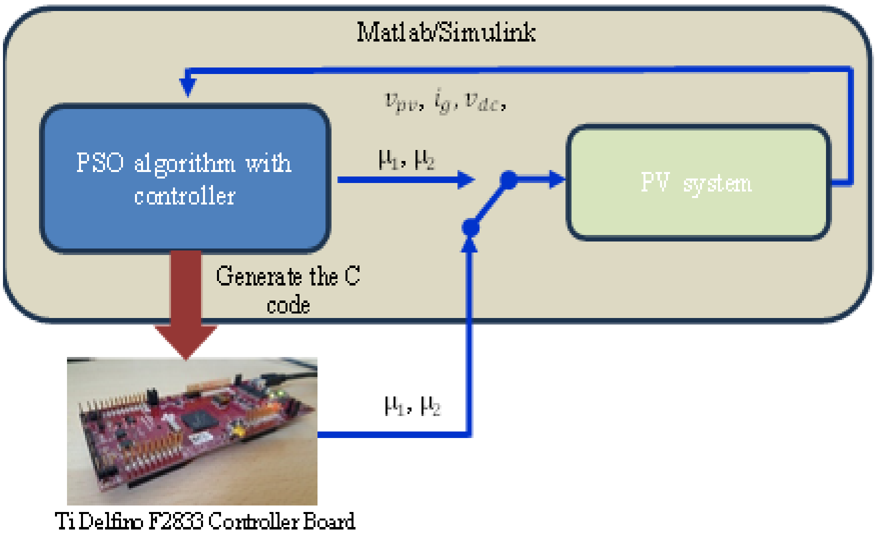

Fig. 3 Block diagram of the PIL implementation process.

ISSN: 2961-6603

10.051103/RES.260605105
Vol.5 Iss.1 pp.47-60 International Journal of Renewable Energy and Sustainability (RES)

TABLE III.
CHARACTERISTICS OF THE CONTROLLED SYSTEM

Parameter	Symbol	Value
PV array	Power	213.15W
	Module	*1STH-215-P*
DC/DC converter	L	2mH
	C_{pv}	4mF
DC/AC converter	C	4mF
Grid filter	L_1	2mH
	r_1	5mΩ
	C	$0{,}5e^{-5}$ F
	L_r	2mH
	r_r	5mΩ
PWM	Switching frequency	10kHz
Grid	AC Source	220V
	L_g	10mH
	r_g	0.7Ω

The implementation of the controlled system calls for the careful selection and tuning of the regulator parameters to ensure optimal performance and stability. The specific numerical values used for these parameters are detailed in Table 4, serving as a reference for replicating and validating the proposed control strategy.

TABLE IV.
CONTROLLER PARAMETERS.

Parameter	Symbol	Value
Voltage Regulator	λ_1	10^3
	λ_2	10^3
PFC Regulator	c_3	10^4
	ρ	40
DC Link regulator	k_p	10^{-6}
	k_i	$4*10^{-7}$

The control structure is illustrated in Figure 4, providing a comprehensive overview of the system's design and functional interactions.

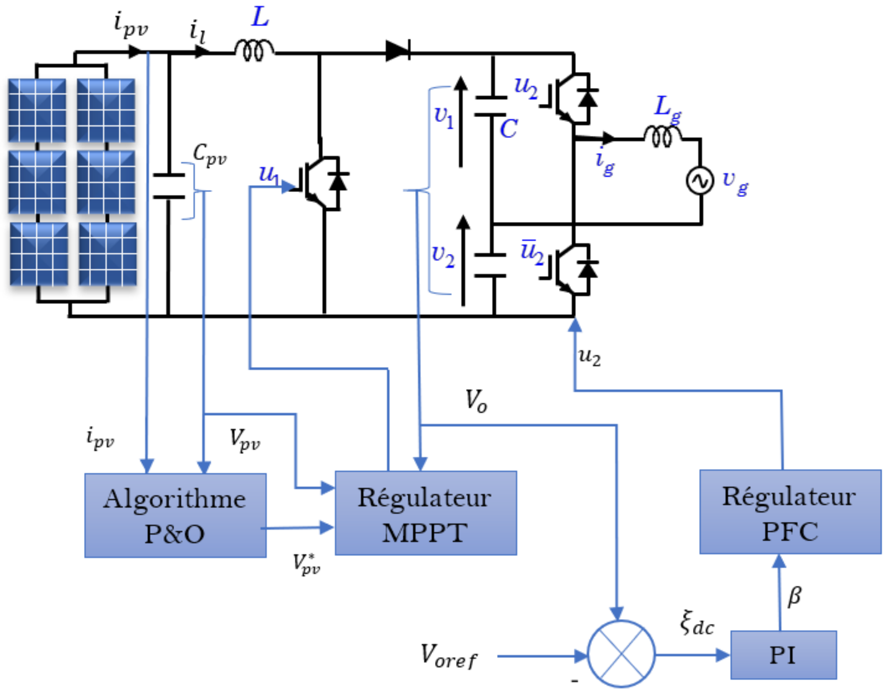

Fig. 4 Control Structure

ISSN: 2961-6603

10.051103/RES.260605105

Vol.5 Iss.1 pp.47-60 **International Journal of Renewable Energy and Sustainability (RES)**

A. Standard Climatic Conditions

Figure 5 illustrates the variation of the PV output voltage, showing that the voltage generated by the PV panels accurately follows its reference determined from the Particle Swarm Optimization (PSO) algorithm. The use of PSO guarantees better performance compared to previously used algorithms such as the P&O used [5].

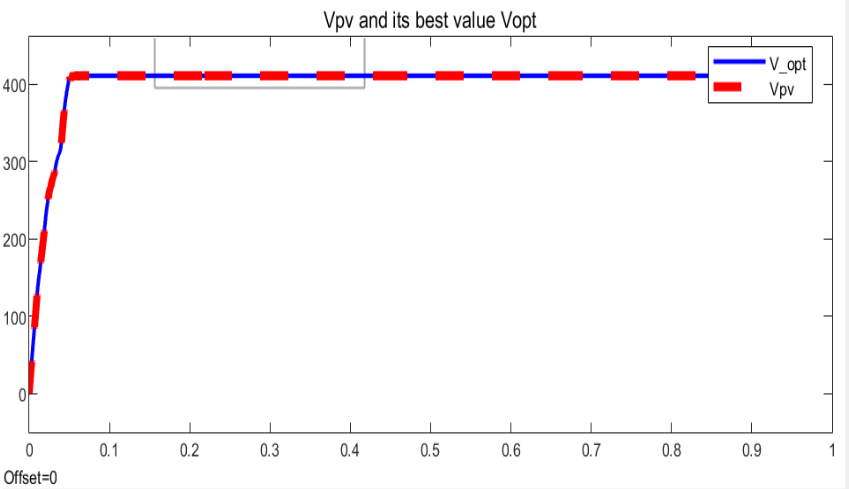

Fig. 5 PV voltage output and its PSO reference

Figure 6 shows the measured DC bus voltage, which accurately converges to the desired reference level of 900 V. The output voltage ripples shown in the figure oscillate at a frequency of $2\pi f_g$, but their amplitudes remain negligible compared to the average value of the signal, which ensures smooth and reliable operation of the system.

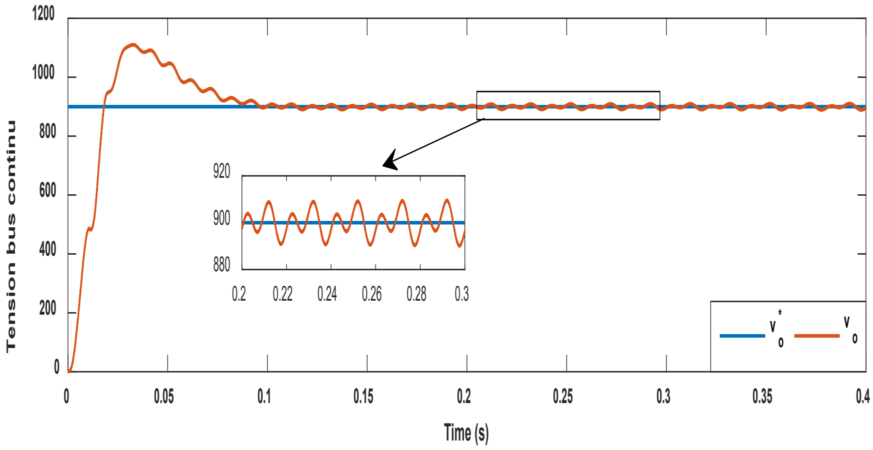

Fig. 6 DC link voltage and the reference

Figure 7 shows that the grid current converges to the desired reference.

ISSN: 2961-6603

10.051103/RES.260605105
Vol.5 Iss.1 pp.47-60 International Journal of Renewable Energy and Sustainability (RES)

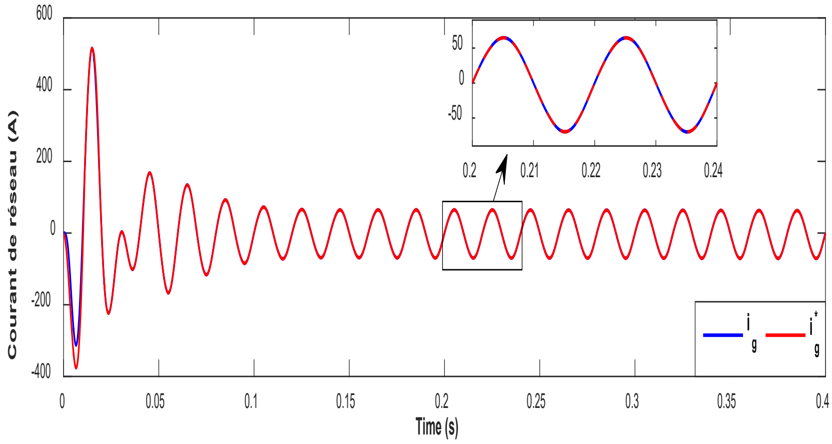

Fig. 7 Grid current and its reference

Figure 8 shows that the grid current and the network voltage are sinusoidal and in phase. This proves that the correction of the power factor is well established.

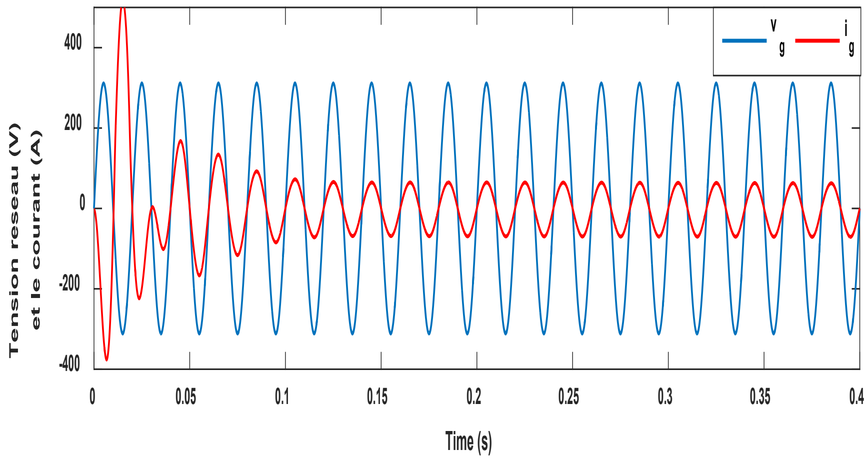

Fig. 8 Grid current and Voltage

B. Temperature Variation Mode

The control performance of the entire system is evaluated under sudden changes in solar temperature. During the simulation, the temperature level increases abruptly from 25°C to 35°C. This scenario tests the system's ability to adapt to dynamic environmental changes while maintaining optimal performance.

In Figure 9 it is clearly seen that thanks to the particle swarm optimization (PSO) algorithm, the controller ensures that the PV voltage accurately tracks the maximum power point, even under large variations in temperature levels.

ISSN: 2961-6603

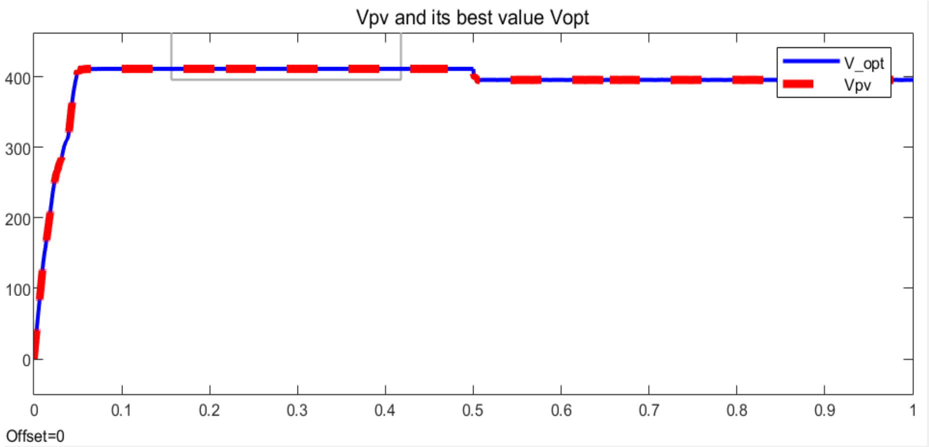

Fig. 9 PV voltage output and its PSO reference

VI. CONCLUSION

In this work, we addressed the nonlinear control problem of a PV system connected to a single-phase grid via a half-bridge inverter using the PSO algorithm for the MPPT. The main control objectives were to achieve the overall maximum and maintain it through the PSO algorithm even under variable climatic conditions, correct the power factor, and regulate the DC bus voltage. The system is modelled with an 5th-order mean-state model. The maximum power point tracking (MPPT) was developed by the particle swarm optimization (PSO) algorithm. This algorithm mimics the collective behaviour of swarms to optimize the PV voltage, ensuring maximum power extraction even under varying irradiance conditions. Based on this model, three control loops were designed using the Backstepping technique and PI corrector. And from the simulation results, it is clearly seen that the proposed controllers, improved by the PSO algorithm, have achieved the control objectives defined above while ensuring the closed-loop stability of the entire system. Experimental validation was carried out using the PIL, and the results obtained match the simulation results, which allows the work to be validated

REFERENCES

[1] Mosallam, H.A., Badran, E.A.. *A Systematic Review of DC–DC Converter Technologies: Traditional, Bidirectional, and Impedance-Source Topologies*. Discover Electronics 3, 16. 2026 https://doi.org/10.1007/s44291-026-00168.
[2] De Brito, M.A.G.; Galotto, L.; Sampaio, L.P.; e Melo, G.d.A.; Canesin, C.A. *Evaluation of the Main MPPT Techniques for Photovoltaic Applications*. IEEE Trans. Ind. Electron. 2013, 60, 1156–1167.
[3] Altin N, Ozdemir S. *Three-phase three-level grid interactive inverter with fuzzy logic based maximum power point tracking controller*. Energy Convers Manag 2013; 69:17–26. https://doi.org/10.1016/j.enconman.2013.01.012.
[4] Abouloifa, A., Aouadi, C., Lachkar, I., Boussairi, Y., Aourir, M., Hamdoun, A.,. *Output-Feedback Nonlinear Adaptive Control Strategy of the Single-Phase Grid-Connected Photovoltaic System*. J. Sol. Energy 2018,
[5] Dammah, H., Lachkar, I., Lissane Elhaq, S., n.d. *Advanced Nonlinear Control of Grid Connected Photovoltaicsystem Based on a Half Bridge Inverter* 12. international journal of control theory and application ISSN: 0974-5572 Volume 1O Number 30 2017, 259-270
[6] Tsang KM, Chan WL. *Model based rapid maximum power point tracking for photovoltaic systems*. Energy Convers Manag 2013; 70:83–9. https://doi.org/10.1016/j.enconman.2013.02.018.
[7] Sakthigokulrajan C, Ravi K. *Combined role of derived array configurations and MPSO based MPPT in improving the energy yield under partial shading conditions*. J Build Eng 2017; 9:125–34. https://doi.org/10.1016/j.jobe.2016.12.006.
[8] BenRegaya C, Hamdi H., Ferhani F., Marai A., Zaafouri A., Chaari A., *Real-time implementation of a novel MPPT control based on the improved PSO algorithm using an adaptive factor selection strategy for photovoltaic systems*. ISA Transactions Volume 146, March 2024, Pages 496-510 https://doi.org/10.1016/j.isatra.2023.12.024
[9] Muhammad N,. Nor Aziyah B., Ahmad S., Nurnaim K., Mohd H., Aimi I., *MPPT Design Using PSO Technique for Photovoltaic System*. IEEE 3rd International Conference in Power Engineering Applications (ICPEA) 10 April 2023 https://doi.org/10.1109/ICPEA56918.2023.10093161
[10] Ali, K., Khan, L., Khan, Q., Ullah, S.,. *Robust Integral Backstepping Based Nonlinear MPPT Control for a PV System*. Energies 12(16), 3180. 2019. https://doi.org/10.3390/en12163180.
[11] Chnini, K., et al., 2024. Enhancing Power Generation via an Adaptive Neuro-Fuzzy and Backstepping Controller for Photovoltaic Systems. Clean Energy 8(5). *2024*. https://doi.org/10.1093/ce/zkae034.

ISSN: 2961-6603

10.051103/RES.260605105
Vol.5 Iss.1 pp.47-60 **International Journal of Renewable Energy and Sustainability (RES)**

[12] Debdouche, N., Benbouhenni, H., Zarour, L., Mehazzem, F., Defaf, B., Chebabhi, A.,. *Nonlinear MPPT Techniques to Control Hybrid Power Systems. Scientific Reports* 14, 18620. 2024. https://doi.org/10.1038/s41598-024-69403-6.
[13] Mosallam, H.A., Badran, E.A.,. *A Systematic Review of DC–DC Converter Technologies: Traditional, Bidirectional, and Impedance-Source Topologies. Discover Electronics* 3, 16. 2026. https://doi.org/10.1007/s44291-026-00168-0.

ISSN: 2961-6603